Draft, in press, *Proc 10th International Conference on Estuarine and Coastal Modeling*, 2007.

Development of A Numerical Model for Simulating Morphodynamic Processes Driven by Tides and Waves at Coastal Inlets

Yan Ding[1] and Sam S. Y. Wang[2]
[1]Ph.D., A.M. ASCE, Research Assistant Professor, [2]Ph.D., P.E., F. ASCE, F.A.P. Barnard Distinguished Professor & Director, National Center for Computational Hydroscience and Engineering, The University of Mississippi, Oxford, MS 38677, Email: ding@ncche.olemiss.edu

ABSTRACT

This paper presents an integrated computational modeling system for simulating tide, storm waves, short wave-induced nearshore currents, wind effects, sediment transport, and morphodynamic processes in coastal zones including coastal inlets and structures (e.g., jetties). An advanced implicit solution scheme has been developed to solve the two-dimensional shallow water equations for simulating coastal hydrodynamics with multiple temporal and spatial scales driven by combined tide, short wave, and wind forcing. Within integration into the Surfacewater Modeling System (SMS), the model's capability to simulate hydrodynamic and morphodynamic processes at a coastal inlet with jetties for both short- and long- term simulation has been confirmed. Through preliminary numerical investigation of the morphological changes around the coastal inlet, it has been found that this coastal modeling system is efficient and robust, and can be generally applicable to simulate morphodynamic processes driven by tides and waves in coastal and estuarine zones with structures.

INTRODUCTION

Understanding coastal morphologic changes due to storm waves and tides is of importance to coastal sediment management, shoreline erosion protection, navigation channel maintenance, design and plan of coastal structures for different engineering purposes, and for coastal environmental impact assessment. Required by the cost-effective designs of coastal engineering projects, computational models have been applied together with physical models to refine and optimize the designs more often than before. Sometimes, computational models have been utilized even exclusively in some cases, when the time available for solving the problems is not enough to build the physical models.

Coastal inlets usually exist along barrier island coasts, which facilitate the exchange of fresh and saline water, and provide a pathway for materials being carried in water including sediments and nutrients (Figure 1). Since barrier islands and inlets bear the brunt of attack by the ocean waves, tides, and storms, they can experience significant beach erosion, sediment transport, bed change of inlet channel, and water exchange, which in turn controls shoreline stability, navigation maintenance, marine ecological and environmental quality, etc. Militello and Kruas (2003) pointed out that common morphodynamic responses to tides and storm waves are characterized by inlet ebb and flood shoals, navigation channel refilling, migration of the inlet channel

thalweg, bypassing at the ebb shoal, skewing of the ebb shoal, development of tip shoals, impoundment at the updrift jetty, beach erosion near the downdrift jetty, and scour holes inside the inlet adjacent to the jetty tips.

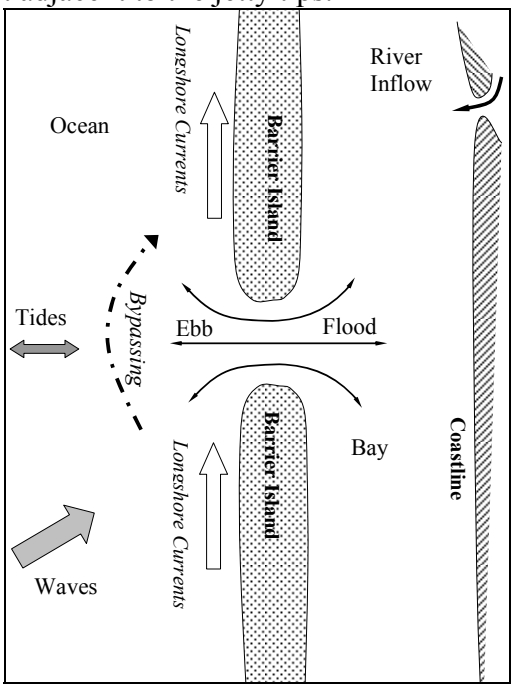

Figure 1 Coastal inlet hydrodynamics

Computational models for simulating tides and short wave-induced currents, as well as short- and long-term morphodynamic change must be capable of representing the complex but important flow characteristics generated by short-period waves from the sea, long-period tides, and nearshore currents with different spatial and temporal scales. To meet the demands, an integrated numerical modeling system for simulating tidal and wave-induced currents has been developed in the National Center for Computational Hydroscience and Engineering (NCCHE) at The University of Mississippi (Ding and Wang 2006a) under the sponsorship of the U.S. Army Corps of Engineers. This circulation model in this system is based on the shallow water equations including forcing by short-wave averaged radiation stresses and the tide. A prediction-correction procedure for solving the shallow water equations was developed for solving the governing equations discretized by the control volume approach. Recently, this coastal process model has been integrated in the Coastal Modeling System (CMS) being developed under the Coastal Inlets Research Program (CIRP) conducted at the U.S. Army Engineer Research and Development Center (ERDC), Coastal and Hydraulics Laboratory (CHL) (Militello et al. 2004; Buttolph et al. 2006; Wang and Ding 2006b). The CMS is designed to simulate combined circulations (currents and water-surface elevations), waves, and morphological change at inlets and nearby areas and operated on desktop computers through operation in the Surfacewater Modeling System (SMS) interface (Zundel 2006).

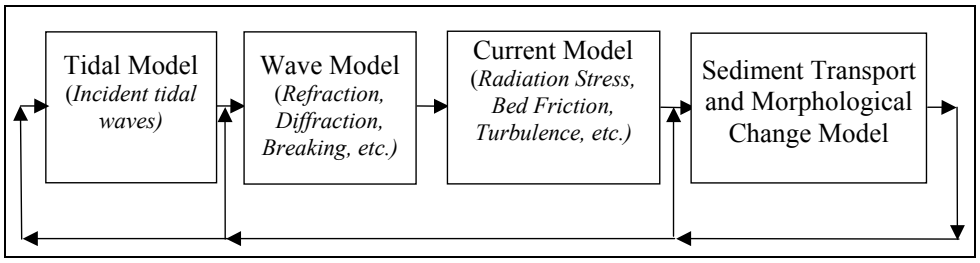

Figure 2 Flow chart of a process-based coastal morphodynamic change model

This integrated coastal morphological model is applied to simulate morphodyanmic changes in a coastal inlet under the actions of waves and tide, by steering (automated interaction) with a spectral wave model in the SMS. A flow chart structure of this integrated CMS model is shown in Figure 2, which consists of four major modules (sub-models), as a spectral wave module, a tide module, a coastal hydrodynamic module for computing tidal and short wave-induced currents, and a sediment transport module. These modules have capabilities of simulating wave parameters (e.g. wave height, period, direction, radiation stress), current driven by the combined tide, waves, and wind, and morphologic changes. The module for simulating morphodynamic processes provides several sub-models, e.g. total sediment load models and suspended sediment transport models, to compute sediment transport rates due to bed load and suspended load.

In this study, the newly developed CMS model's capabilities of representing combined tidal and wave-induced currents in a coastal inlet is confirmed, for which a hypothetical inlet with realistic spatial scale was designed to represent basic geometry, inlet entrance configuration, offshore slope, and wave and tidal forcing at a medium-size inlet such as Shinnecock Inlet, Long Island, New York, located on the US Atlantic coast. The currents were assumed to be subjected to constant spectral waves and constituent tide. The spectral waves which represent the natural random waves were simulated by the CMS-Wave model (Lin et al 2006), which is provided in the SMS. The numerical results correctly reproduce expected trends in morphologic change observed at coastal inlets. Through the preliminary investigation of the idealized coastal inlet, it has been found that the proposed algorithm and numerical approaches are capable of simulating the combined tides and short wave-induced currents, as well as morphodynamic changes in coastal inlets. In addition, because the developed numerical scheme allows a large time step, numerical simulations are computationally efficient and stable.

MODEL DESCRIPTION

Coastal Hydrodynamic Model

In the CMS coastal hydrodynamic model, the depth- and short wave- averaged 2-D continuity and momentum equations are used for simulating currents driven by tides and waves in coastal zones, which are rewritten into a vector form as follows:

$$\frac{\partial \eta}{\partial t} + \nabla \bullet h\mathbf{u} = 0 \tag{1}$$

$$\frac{\partial h\mathbf{u}}{\partial t}+\nabla\bullet h\mathbf{uu}=-gh\nabla\eta+\nabla\bullet(h\mathbf{D}\nabla\mathbf{u})-\frac{1}{\rho}\nabla\bullet\mathbf{R}+\frac{\boldsymbol{\tau}^{S}-\boldsymbol{\tau}^{b}}{\rho}+h\mathbf{f}_{Col} \quad (2)$$

where η = water elevation deviation from the still water level; h = water depth; $\boldsymbol{u}$ = (u_x, u_y), depth- and short wave- averaged velocity vector in the horizontal coordinates; g = acceleration of gravity; $\boldsymbol{D}$ = mixing coefficient; ρ = water density; $\boldsymbol{R}$ = radiation stress which represents the net (short wave-averaged) force the short wave exert on a water column; $\boldsymbol{\tau}^S$ = surface wind stress; $\boldsymbol{\tau}^b$ = bottom friction stress; $\boldsymbol{f}_{\text{col}}$ = (fu_x, $-fu_y$), Coriolis force , $f= 2\Omega sin\varphi$, Coriolis parameter; Ω = angular frequency of earth rotation; φ = latitude.

For irregular waves and a coordinate system with the x-axis oriented normal to the shoreline, the tensor components of the short wave-averaged wave stresses $\boldsymbol{R}$ in the momentum equations (2) are

$$R_{xx}=\frac{1}{2}\iint E(\omega,\alpha)\left[(1+G)(\cos^2\alpha+1)-1\right]d\omega d\alpha \quad (3)$$

$$R_{xy}=\frac{1}{4}\iint E(\omega,\alpha)(1+G)\sin 2\alpha\, d\omega d\alpha \quad (4)$$

$$R_{yx}=R_{xy} \quad (5)$$

$$R_{yy}=\frac{1}{2}\iint E(\omega,\alpha)\left[(1+G)(\sin^2\alpha+1)-1\right]d\omega d\alpha \quad (6)$$

where ω = angular frequency of the short wave; α = wave direction; $E = E(\omega, \alpha)$, wave energy density; and

$$G=\frac{2kh}{\sinh 2kh} \quad (7)$$

where k = wave number. The radiation stresses are calculated by means of linear wave theory and computed by the CMS-Wave model (Lin et al 2006).

For the situation without waves, the bottom friction stresses $\boldsymbol{\tau}^b$ can be represented by the quadratic bottom friction stresses which can be calculated by Manning's roughness coefficient and local water depth. In the case of simulating wave-induced currents, the calculation of the bottom friction stresses has to take into account the bottom orbital motions of the waves. The model uses Nishimura's approximation (Nishimura 1988) to calculate the short wave-averaged bottom friction stress under combined currents and waves. The surface wind stresses $\boldsymbol{\tau}^S$ are given by the empirical wind shear stress formulations (Militello et al. 2004).

Assuming that the depth-averaged eddy viscosity is horizontally homogenous, in order to represent the different diffusion features between the surf zone and the deep water, two different eddy viscosity coefficient formulations are provided respectively in the two zones. In the deep water, suppose that waves do not contribute significantly to the turbulence mixing, this eddy viscosity is calculated by using the local water depth and bottom friction velocity (Falconer 1980). In the surf zone, wave-induced mixing is dominant. The coefficient in the surf zone therefore is calculated according to the formulation proposed by Kraus and Larson (1991). In the transition zone between the surf zone and the deep water, a weighted mixing coefficient is formed to calculate the mixing coefficient (Militello et al. 2004), i.e.

$$D = (1-\theta)D_O + \theta D_W \tag{8}$$

where D_O is calculated by using Falconer's formulation; D_w is done by Kraus-Larson' formulation; and θ= the weighting parameter determined by the ratio of the local wave height to the local water depth.

Sediment Transport and Morphodynamic Change Models

The variation of the seabed elevation Z_b is calculated by considering the local sediment balance and the downslope gravitational transport:

$$\frac{\partial Z_b}{\partial t} = -\nabla \bullet \mathbf{q} + \nabla \bullet (D_S \,|\, \mathbf{q} \,|\, \nabla Z_b) \tag{9}$$

where $\boldsymbol{q}$=(q_x,q_y) is the local sediment transport rate flux consisting of two components in x- and y-directions in the horizontal plane, and D_s is an empiric coefficient to represent the downslope gravitational effect. The bed evolution is described by a divergence term at the right hand side and the other two terms for the downstream gravitational effect. De Vriend et al. (1993) pointed out that this slope-related transport mechanism enables a coastal profile to reach the equilibrium bed topography; otherwise the morphodynamic simulation only based on the law of mass balance (i.e. without the downslope effect) encounters an inherent instability of bed evolution. An Eulerian forward explicit scheme is used in the present CMS morphodynamic model to solve Eq. (9) (Buttolph et al. 2006). In this study, the Lund-CIRP total load sediment transport formulations (Camanen and Larson 2007) provided in the CMS model are used for calculating the total sediment rate including bed load and suspended sediment load. According to the formulations originally proposed by Camenen and Larson (2005), the local sediment transport rate flux has two contributions from bed material and suspended sediments under the conditions of wave and current, i.e.

$$\mathbf{q} = \mathbf{q}_b + \mathbf{q}_s \tag{10}$$

where $\boldsymbol{q}_b$ and $\boldsymbol{q}_s$ are the local sediment transport rates contributed by bed materials and suspended sediments, respectively. A general transport formula for bed load $\boldsymbol{q}_b$ under combined waves and current developed by Camenen and Larson (2005) is adopted to calculate the bed load flux:

$$\frac{q_{bw}}{\sqrt{(s-1)gd_{50}^3}} = a_w \sqrt{\theta_{net}}\,\theta_{cw,m} \exp\left(-b\frac{\theta_{cr}}{\theta_{cw}}\right) \tag{11}$$

$$\frac{q_{bn}}{\sqrt{(s-1)gd_{50}^3}} = a_n \sqrt{\theta_{cn}}\,\theta_{cw,m} \exp\left(-b\frac{\theta_{cr}}{\theta_{cw}}\right) \tag{12}$$

where subscripts w and n refer to the wave direction and the direction normal to the waves, respectively; d_{50} = median grain diameter, and θ_{cr} = critical Shields parameter; and s = specific density, = ρ_s/ρ, where ρ_s= sediment density; a_w, a_n, and b are empirical coefficients, and $\theta_{cw,m}$ and θ_{cw} are the mean and maximum Shields parameters for waves and current combined, respectively. The quantities θ_{net} and θ_{cn} represent the net contribution of the shear stress to the transporting velocity during a wave cycle in the direction parallel and normal to the waves, respectively.

The suspended load $\boldsymbol{q}_s$ is calculated based on the assumptions of an exponential concentration profile and a constant velocity over the water column to yield (Camenen and Larson 2007):

$$\mathbf{q}_s = \mathbf{u} c_R \frac{\varepsilon}{w_S}\left(1-\exp\left(-\frac{w_S h}{\varepsilon}\right)\right) \tag{13}$$

where w_S = sediment settling velocity, c_R = reference concentration, and ε = sediment diffusivity (or turbulence mixing coefficient). The transport $\boldsymbol{q}_s$ is taken to be in the direction of the current because the waves are assumed to produce a zero net drift and not contribute to the suspended sediment transport.

IMPLICIT SOLUTION SCHEME FOR HYDRODYNAMIC MODEL

Prediction and Correction to Solve the Shallow Water Equations

Eqs. (1) and (2) are time-dependent and strongly nonlinear in simulations of coastal hydrodynamics. To gain efficient computational performance, these equations need to be solved in a numerically implicit fashion. Using an Eulerian backward solution scheme to approximate numerically the acceleration term in Eq. (2), a semi-implicit analytical form of the momentum equations can be written as follows:

$$\frac{(h\mathbf{u})^{n+1}-(h\mathbf{u})^{n}}{\Delta t}+\nabla\bullet(h\mathbf{u}\mathbf{u})^{n}=-g(h\nabla\eta)^{n+1}+\nabla\bullet(h\mathbf{D}\nabla\mathbf{u})^{n}-\frac{1}{\rho}\nabla\bullet\mathbf{R}^{n+1}+\frac{\boldsymbol{\tau}^{S(n)}-\boldsymbol{\tau}^{b(n)}}{\rho}+h\mathbf{f}_{col}^{n} \tag{14}$$

where Δt is a time increment; the superscripts n and $n+1$ denotes the nth and $(n+1)$th time step, respectively. Due to its strong nonlinearity, an iterative algorithm is proposed accordingly: Suppose that the water elevation at the $(n+1)$th step is split into two terms:

$$\eta^{n+1}=\eta^{*}+\eta' \tag{15}$$

where the superscript star * means an estimated value; the prime denotes a correction value. Provided that an estimated velocity can be calculated by the following momentum equations:

$$\frac{(h\mathbf{u})^{*}-(h\mathbf{u})^{n}}{\Delta t}+\nabla\bullet(h\mathbf{u}\mathbf{u})^{n}=-g(h\nabla\eta)^{*}+\nabla\bullet(h\mathbf{D}\nabla\mathbf{u})^{n}-\frac{1}{\rho}\nabla\bullet\mathbf{R}^{n+1}+\frac{\boldsymbol{\tau}^{S(n)}-\boldsymbol{\tau}^{b(n)}}{\rho}+h\mathbf{f}_{col}^{n} \tag{16}$$

comparing (16) with (14), assuming that h^{*} is close to h^{n+1}, therefore,

$$(h\mathbf{u})^{n+1}=(h\mathbf{u})^{*}-\Delta t g h^{*}\nabla\eta' \quad \text{or} \quad \boldsymbol{u}^{n+1}=\boldsymbol{u}^{*}-\Delta t g\nabla\eta' \tag{17}$$

Because the solutions of velocities should satisfy with the continuity equation (1) at the $(n+1)th$ step, i.e.

$$\left(\frac{\partial\eta}{\partial t}\right)^{n+1}+\nabla\bullet(h\mathbf{u})^{n+1}=0 \tag{18}$$

by substituting (17) into (18), an equation about the water elevation correction is obtained readily,

$$\nabla\bullet(\Delta t g h^{*}\nabla\eta')=\left(\frac{\partial\eta}{\partial t}\right)^{n+1}+\nabla\bullet(h\mathbf{u})^{*} \tag{19}$$

Note that

$$\left(\frac{\partial\eta}{\partial t}\right)^{n+1}=\frac{\eta^{n+1}-\eta^{n}}{\Delta t}=\frac{\eta^{*}-\eta^{n}}{\Delta t}+\frac{\eta'}{\Delta t} \tag{20}$$

Eq. (19) then becomes

$$\nabla \bullet (\Delta t g h^* \nabla \eta') - \frac{\eta'}{\Delta t} = \frac{\eta^* - \eta^n}{\Delta t} + \nabla \bullet (h\mathbf{u})^* \tag{21}$$

This is a Poisson equation about the water elevation correction η'. In the solution procedure, once the estimated velocities and the water elevations are obtained, the elevation correction is calculated by Eq. (21).

An Implicit Time-Marching Algorithm for Solving the Shallow Water Equations

Ding and Wang (2006b) developed an implicit time-marching algorithm to solve coastal hydrodynamics governed by the nonlinear and time-dependent shallow water equations in coastal inlets and adjacent shores. The numerical test results indicated that this implicit scheme has a high efficiency in computations of the currents under the combined forcing of waves and tides. The analytical form of the algorithm is summarized as follows:

Step 1: Given variables $\boldsymbol{u}^n$ and η^n at the nth time step;

Step 2: Obtain provisional velocities $\boldsymbol{u}^*$ by implicitly solving the following momentum equations at the $(n+1)$th time step:

$$\frac{(h\mathbf{u})^* - (h\mathbf{u})^n}{\Delta t} + \nabla \bullet (h\mathbf{u}\mathbf{u})^* = -gh\nabla \eta^* + \nabla \bullet (h\mathbf{D}\nabla \mathbf{u}^*) - \frac{1}{\rho}\nabla \bullet \mathbf{R}^{n+1} + \frac{\boldsymbol{\tau}^{S(n)} - \boldsymbol{\tau}^{b(n)}}{\rho} + h\mathbf{f}_{col}^n \tag{22}$$

Step 3: Solve the Poisson equation (21) of the water elevation correction η' ;

Step 4: Correct velocities using Eq. (17) and the correction values of the water elevations. Update the water elevations η^{n+1} by Eq. (15) ;

Step 5: If the accuracy of $\boldsymbol{u}^{n+1}$ and η^{n+1} satisfies the continuity equation, go to Step 6. Otherwise, replace $\boldsymbol{u}^*$ and η^* by $\boldsymbol{u}^{n+1}$ and η^{n+1}, respectively. Then, go to Step 2 to re-compute velocities and water elevations.

Step 6: Compute the sediment fluxes due to bed load and suspended sediment transport. And compute the morphodynamic change by Eq. (9). Then, go to step 1 for the computation at a new time step.

This algorithm contains an iterative cycle of prediction and correction to assure that the computed velocities and water elevations are satisfied with the continuity equation. In terms of extensive tests for the numerical model, it is found that the developed implicit numerical scheme is stable and robust to simulate the highly-nonlinear shallow water equations with the combined wave and tidal forcing; only a limited number of the iterations for prediction and correction in each time step. For example, the total number of 10 iterations was found to be the maximum iteration number for most real coastal inlet problems. Moreover, a large time increment can be used and therefore highly efficient computational performance can be obtained (Ding and Wang 2006b).

FULLY-IMPLICIT DISCRETIZATION BY CONTROL VOLUME APPROACH

The previous CMS numerical model was built in a rectangular grid mesh in the Cartesian coordinates. Herein, the physical variables in the newly developed implicit CMS model are located in a staggered mesh. A typical control volume cell is shown

in Figure 3, in which the nodes marked by circles are to define the water elevations; the velocity components indicated by arrows are located at the control volume interfaces. In the early 1970s, Patankar (1980) successfully employed a staggered mesh to develop a well-known numerical algorithm, SIMPLE (Semi-Implicit Method for Pressure-Linked Equations). Since then, the staggered arrangement of control volume cells has been widely used in various CFD software packages for simulations of fluid flows, for example, MIKE21 (MIKE21 2006; Zyserman and Johnson 2002), DELFT3D (Lesser et al. 2004), and POM (Mellor 1998).

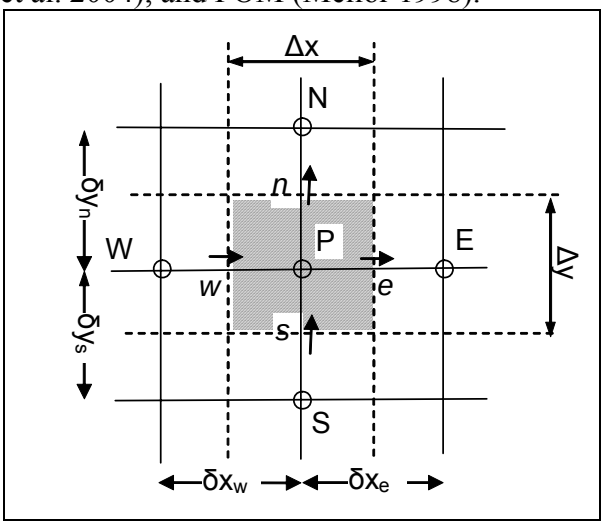

Figure 3 Various measures in a general control volume cell

Although the cells for the velocities in *x*- and *y*-directions are arranged in two staggered grids, the momentum equations (2) still can be discretized as the following general penta-diagonal linear algebraic equations, i.e.

$$a_P\varphi_p = a_W\varphi_W + a_E\varphi_E + a_S\varphi_S + a_N\varphi_N + S_\varphi \tag{23}$$

where φ is a general variable representing the velocities in *x*- and *y*-directions; S_φ is a source term which is different in the two equations. The coefficients in (23) are directly given as follows:

$$a_p = a_W + a_E + a_S + a_N + h\Delta x\Delta y/\Delta t \tag{24}$$

$$a_W = D_w A(P_w) + Max[F_w, 0], \quad a_E = D_e A(P_e) + Max[-F_e, 0] \tag{25}$$

$$a_S = D_s A(P_s) + Max[F_s, 0], \quad a_N = D_n A(P_n) + Max[-F_n, 0] \tag{26}$$

$$F_w = (hu)_w \Delta y, \qquad F_e = (hu)_e \Delta y \tag{27}$$

$$F_s = (hu)_s \Delta x, \qquad F_n = (hu)_n \Delta x \tag{28}$$

$$D_w = (hD_\phi)_w \Delta y/\delta x_w, \qquad D_e = (hD_\phi)_e \Delta y/\delta x_e \tag{29}$$

$$D_s = (hD_\phi)_s \Delta x/\delta y_s, \qquad D_n = (hD_\phi)_n \Delta x/\delta y_n \tag{30}$$

where Δx and Δy are respectively cell length and width; $A(P)$ is a function of the Peclet number P, which is defined as F/D. An upwinding scheme can be adopted if $A(P) = 1$; or an exponential scheme if $A(P) = Max[0, (1-0.1|P|)^5]$ (Patankar1980). Moreover, the source terms S_Φ, e.g. the bottom friction terms, need to be linearized respectively for the two momentum equations. The negative linear terms in the source terms can be added up to the a_p coefficient.

Similarly, the water elevation correction equation (21) also can be integrated in a control volume cell shown in Figure 3. A similar penta-diagonal linear algebraic equation can be obtained:

$$a_P \eta'_P = a_W \eta'_W + a_E \eta'_E + a_S \eta'_S + a_N \eta'_N + b \tag{31}$$

where the coefficients and the source term *b* are given as:

$$a_W = \Delta t g h_w \Delta y / \delta x_w, \qquad a_E = \Delta t g h_e \Delta x / \delta y_e \tag{32}$$

$$a_S = \Delta t g h_s \Delta x / \delta y_s, \qquad a_N = \Delta t g h_n \Delta x / \delta y_n \tag{33}$$

$$a_p = a_S + a_W + a_E + a_N + \Delta x \Delta y / \Delta t \tag{34}$$

$$b = \left[(hu)^*_w - (hu)^*_e \right] \Delta y + \left[(hv)^*_s - (hv)^*_n \right] \Delta x - (\eta^* - \eta^n) \Delta x \Delta y / \Delta t \tag{35}$$

The penta-diagonal linear algebraic equations for velocities in (23) and water elevation corrections in (31) are solved by the strong implicit procedure (SIP) proposed by Stone (1968).

MORPHODYNAMIC SIMULATIONS OF IN COASTAL INLETS

This implicit coastal hydrodynamic model has been developed and integrated into the CMS, which is being actively developed and upgraded to calculate combined circulations (current and water-surface elevation), waves, and morphological changes at inlets and nearby areas and operated on desktop computers through operation in the SMS interface (Zundel 2006). To investigate morphodynamic responses to variations in jetty configuration (equal-length and offset jetties), different wave conditions (small waves and storm waves), and short- and long-terms, the CMS simulations have been performed in an idealized inlet with a 300-m width channel (Figure 4a) that abstracts basic geometry, depth, inlet entrance configuration, offshore slope, grain size, and wave and tidal forcing, but without developed ebb and flood shoals. Therefore, the initial bathymetry of the idealized inlet may be similar to a newly opened coastal inlet (Figure 4b).

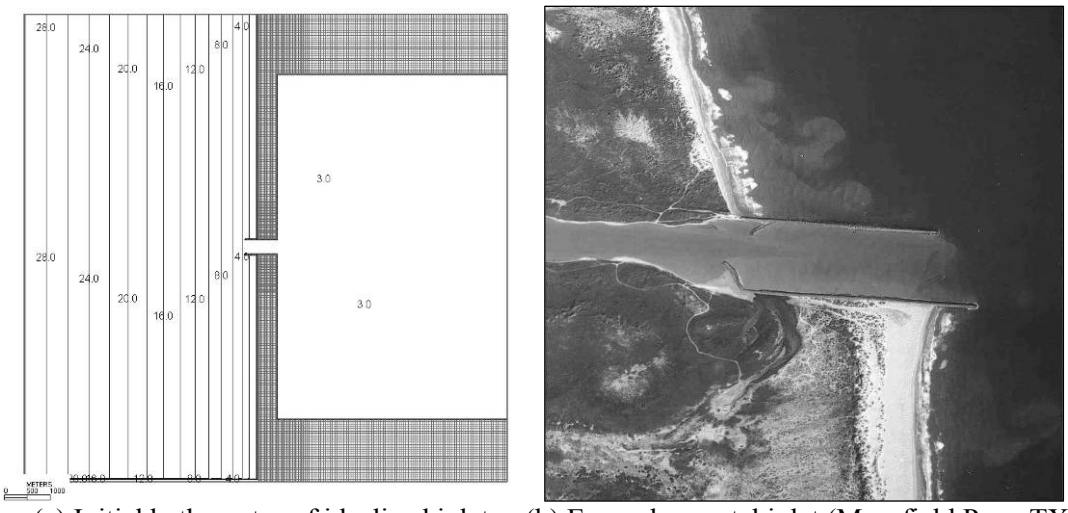

(a) Initial bathymetry of idealized inlet (b) Example coastal inlet (Mansfield Pass, TX)

Figure 4 Idealized inlet with features similar to a typical coastal inlet

The morphodynamic simulations were carried out for two cases with two different jetty configurations, dual jetties of equal length (250 m) and offset jetties (downdrift jetty shortened by 125 m). The wave-current-morphology interaction was controlled by the steering module of the SMS interface with 3-hr interval. The computed currents and water elevations were fed back to the recalculation of the wave variables (i.e., so-called two-way steering run). The time step size in simulating currents was 60 s. The uniform grain size in the coast was 0.2 mm. A total load sediment formula, the Lund-CIRP formula, was applied to compute the total sediment transport rate. Then, Eq. (9) was adopted to compute the bed elevation changes by using an explicit Eulerian forward difference scheme.

Long-term Morphodynamic Simulation Driven by Small Waves and Tides

As a first step, starting from the initial bathymetry shown in Figure 4(a), the morphodynamic simulations were performed for the two cases which were subject to constant spectral waves representing a fair weather condition (1.5 m and 8 s significant height and period, incident 30 deg from the SW, and JONSWAP spectrum) and a M_2 tide (range of 1 m) for more than one month. The wave model in the steering runs was the CMS-Wave model (Lin et al 2006). The purpose by this step was to create natural coastal bathymetries around the inlets by going through long-term morphodynamic processes driven by the fair weather wave condition. As shown in Figure 5, the computed bed elevations in the two cases at the 35th day present new bathymetries with ebb shoal, flood shoal, and uneven channel bed, which are similar to natural coastal geomorphologic conditions commonly appearing at inlets. The two cases, which have two different jetty configurations, created almost same formations about ebb and flood shoals. The water depths at the ebb shoals are slightly different from, i.e., 3.0-m deep ebb shoal found in the inlet with dual equal-length jetties, and 2.5-m deep ebb shoal in the second one with offset jetties.

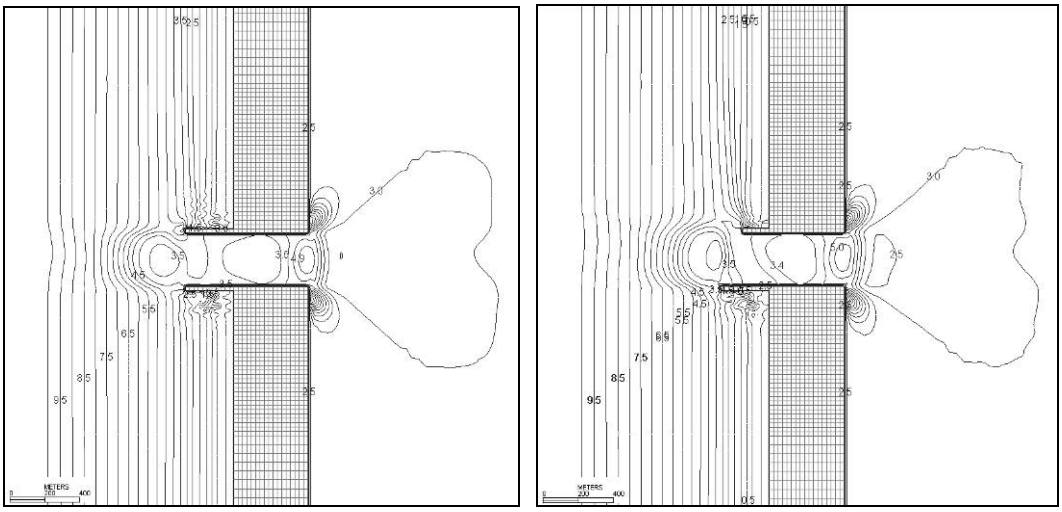

(a) Dual jetties of equal length (b) Offset jetties

Figure 5 Computed bed elevations at 35th day

Short-term Morphodynamic Simulations Driven by Storm Waves and Tides

After bathymetries were created around the two coastal inlets close to a natural condition, which contained several principal features of a coastal inlet, such as ebb shoals, flood shoals, and scouring in the tips of the jetties, further simulations of morphodynamic processes for the two cases started at the two simulation-generated bathymetries. Assuming that the coastal inlets were attacked by storm waves, this step of morphodynamic simulation was to investigate the morphological changes at and near the inlets caused by storm waves during a short-term (typically several days). A constant spectral storm waves at offshore were 3.5 m and 9 s significant height and period, incident at 30 deg from the SW, which was defined as a JONSWAP spectrum with the parameter γ=3.3. The currents were assumed to be subject to a M_2 tide (range of 1.0 m). Similar to the first step of the morphodynamic simulations, the coastal hydrodynamics was computed by using a 60-s time increment; the wave fields were recomputed after every 3-hr hydrodynamic simulation with a two-way steering run.

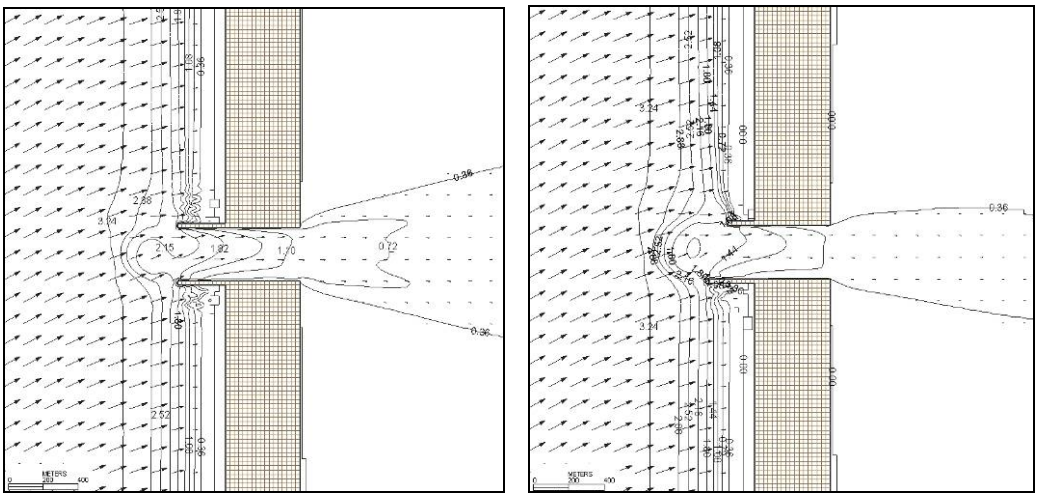

(a) Dual jetties of equal length (b) Offset jetties

Figure 6 Computed wave heights and directions at flood tide

Figure 6 (*a*) and (*b*) show the wave heights and directions at a flood tide for the two cases, respectively. Strong refraction, wave shoaling, and breaking occur at and near the ebb shoals. The computed breaking wave was approximately 2.0-m high at the ebb shoal of the coast with the equal-length jetties (Figure 6a), and 1.5-m high at the ebb shoal of the second one (Figure 6b).

Several snapshots of the computed currents and bed elevations during the storm period are shown in Figure 7 - Figure 10. At a slack tide shown in Figure 7, the obliquely incident wave (30 degree from SW) skew the longshore currents to the north, which make the ebb shoals asymmetric. Flowing over the ebb shoal, the longshore currents bypass the inlet channel toward the north. On the other hand, due to the longer down-drift jetty, the recirculation zone in the dual jetties of equal length is much larger than that in the offset jetties. The bypass currents may directly erode the sand at the tip of the shortened jetty, and then cause the beach erosion near the down-drift jetty. At an ebb tide shown in Figure 8, the longshore currents from the south are carried along with strong ebb currents. However, because of the shortened

jetty, the ebb currents in the second case almost turn toward the north; some of the currents quickly reattach to the beach near the shortened jetty. When the strength of ebb currents decreases, as shown in Figure 9, the longshore currents from the south form a peripheral current around each ebb shoal in the two cases. Then the ebb currents are incorporated into the bypassing longshore currents flowing toward the north. It can make the longshore currents near the north beach stronger than those in the south. At a strong flood tide in Figure 10, both the flood current and the longshore currents from the south flow into the bay. However, in the inlet with the offset jetties, the flood current inside the channel decelerate at the entrance of the longer jetty; this can make sand deposited at the channel entrance. Meanwhile, the current at the tip of the shortened jetty (Figure 10b) becomes much faster than that in the longer downdrift jetty in the first case with the dual equal-length jetties (Figure 10a). It can cause more erosion at the root of the shortened jetty, and more scouring at the tip.

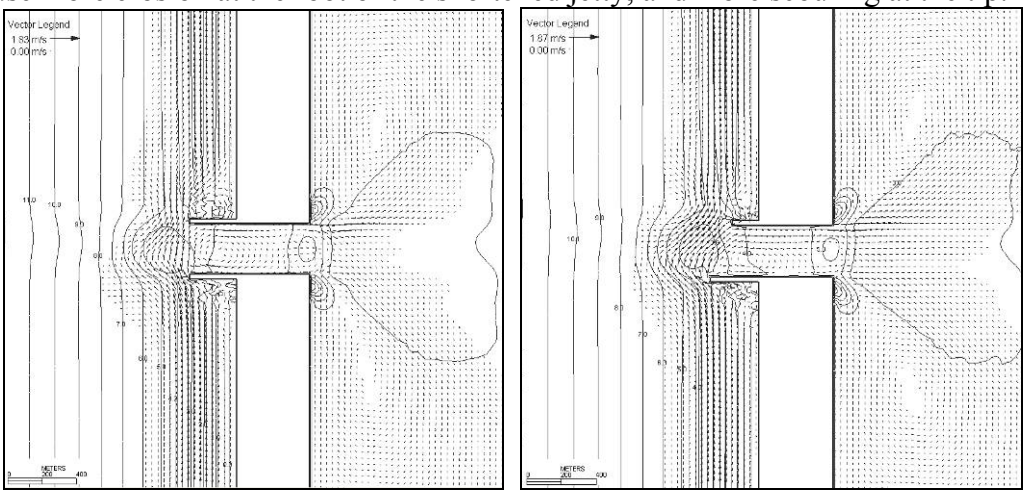

(a) Dual jetties of equal length (b) Offset jetties

Figure 7 Current and bed elevations computed at t=39 hr, slack tide.

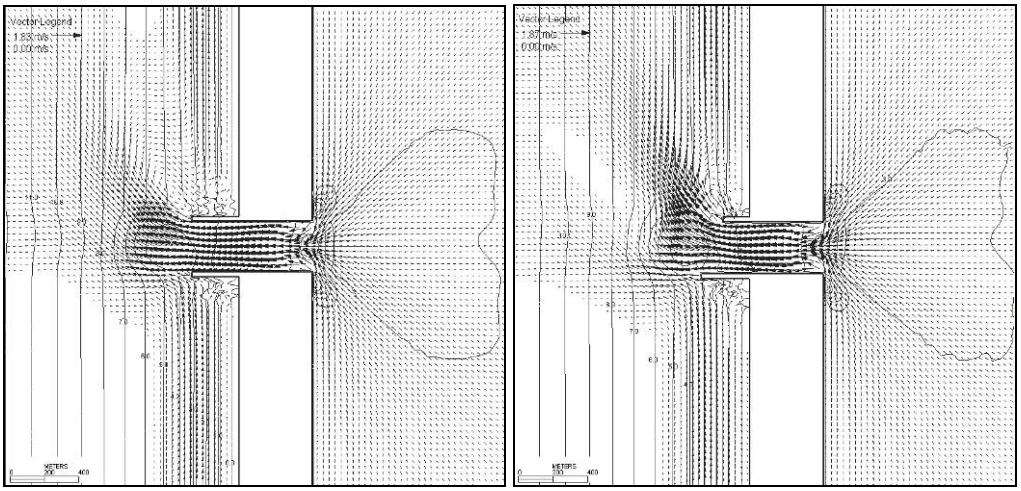

(a) Dual jetties of equal length (b) Offset jetties

Figure 8 Current and bed elevations computed at t=42 hr, ebb tide.

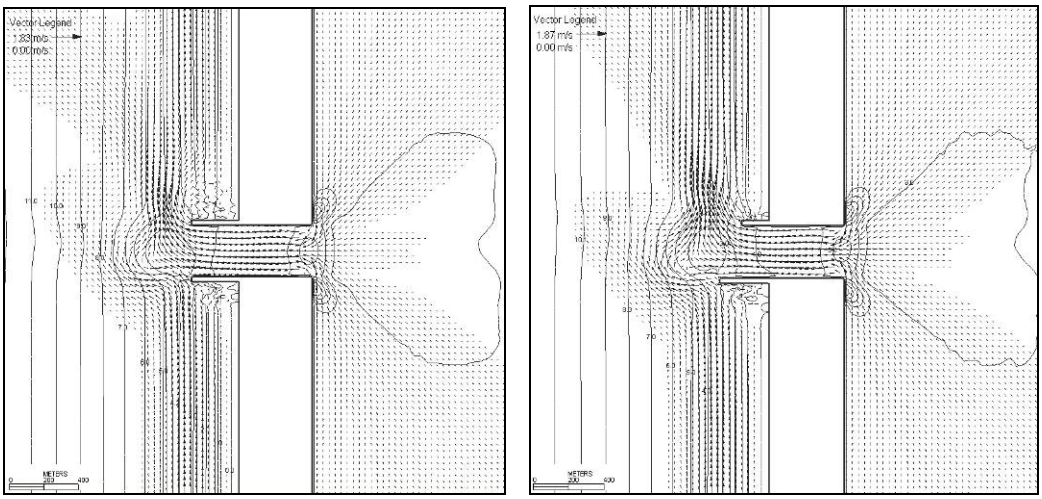

(a) Dual jetties of equal length (b) Offset jetties

Figure 9 Currents and bed elevations computed at t=45hr, ebb tide.

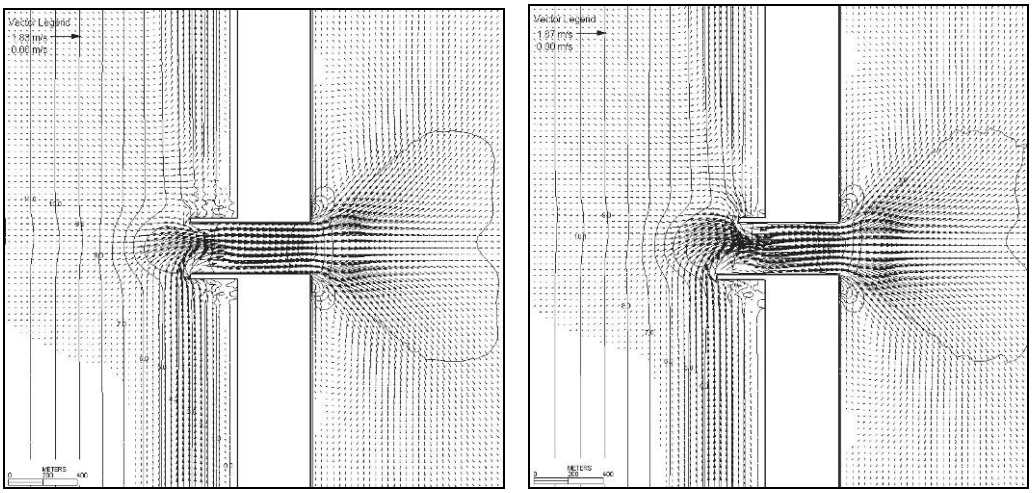

(a) Dual jetties of equal length (b) Offset jetties

Figure 10 Currents and bed elevations computed at t=48hr, flood tide.

Figure 11 and Figure 12 present the computed bed change and sediment fluxes at 45 hr (an ebb tide), and 48 hr (a flood tide), respectively, in which the dark gray color indicates deposition (or formation of bar), the light or white color represents erosion (scour). The two pictures in Figure 11 show clearly the bypassing sediments form updrift bar and bypass bar at the downdrift side in both the two cases. Due to the attack of the storm waves, the ebb shoals created in the fair weather season are found to be eroded. Some of sands can move into the channel, and deposit in the channel, which may lead to channel refilling problem. As shown in the figures, the scours can be found in the tips of the jetties and inside the channel. Apparently, the erosion area in the shortened downdrift jetty is likely expanded toward the beach near the root of the jetty as long as the storm wave retains the strength further longer. In other words, the offset jetties can cause more severe erosions locally around the downdrift jetty than those in the dual equal-length jetties.

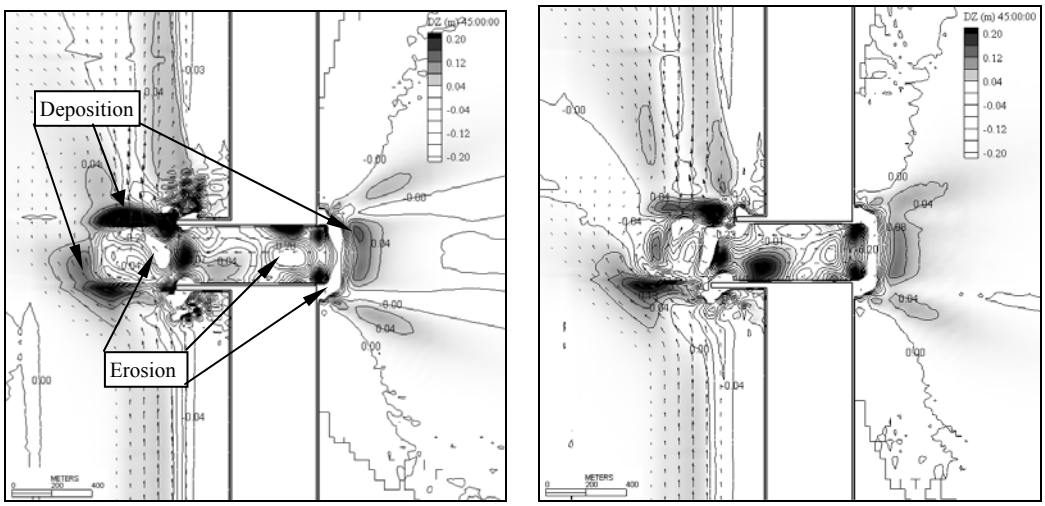

(a) Dual jetties of equal length (b) Offset jetties

Figure 11 Computed bed changes and sediment fluxes at t = 45 hr, ebb tide

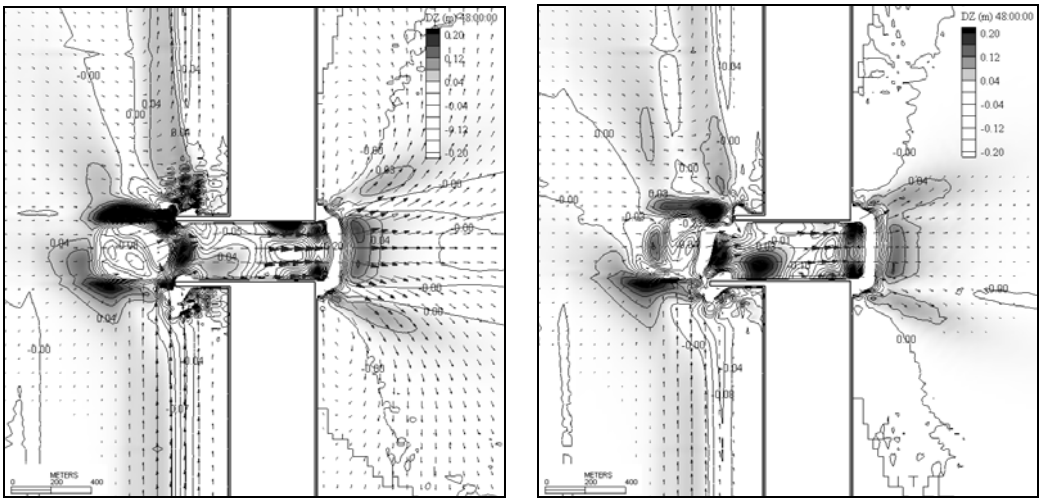

(a) Dual jetties of equal length (b) Offset jetties

Figure 12 Computed bed change and sediment fluxes at t = 48 hr, flood tide

To quantify the changes of the ebb shoals, Figure 13 presents the two profiles of the bed elevations along a cross-section through the inlet channel after the storm waves. The results show that the ebb current through the equal-length jetties can push the ebb shoal further offshore than that by the offset jetties; but the flood shoal for the equal-length jetties develops at a slightly slower rate than for the offset jetties.

CONCLUDING REMARKS

A new computational model for the CMS modeling system has been developed to simulate tidal and short wave-induced currents, as well as morphological changes in coastal inlets and their adjacent coasts. To provide an efficient and robust coastal model, an implicit solution scheme with prediction-correction procedure was developed and applied to solve the two-dimensional shallow water equations for

simulating coastal hydrodynamics with multiple temporal and spatial scales driven by the combined tides and shortwave radiation stresses. With integration into the SMS, the capabilities of the CMS to simulate hydrodynamic and morphodynamic processes at coastal inlets with different jetty configurations was confirmed. The computed bed elevation changes demonstrated clearly that the simulated bathymetries consist of the development of ebb and flood shoals, scour at the jetty tips, the sediment deposition in the channel, and sand bypassing between the inlet jetties. These numerical results correctly responded the morphological changes commonly observed at coastal inlets. Through this preliminary numerical investigation of the morphologic change around coastal inlets, it has been found that this newly-developed coastal computational model indeed performs efficiently and robustly, and is generally applicable to simulate morphodynamic processes driven by tides and waves in coastal and estuarine zones with structures. However, by using accurate and reliable field and laboratory measurement data, validation of CMS capabilities in predicting coastal morphodynamic processes is recommended.

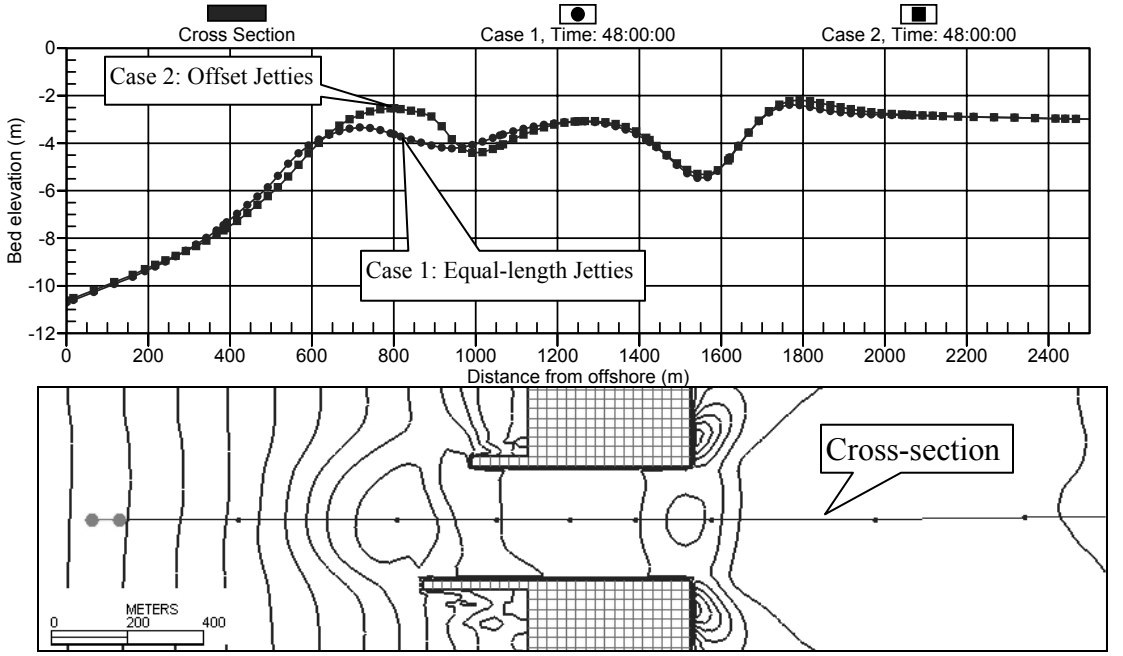

Figure 13 Comparison of profiles of bed elevations along a cross-section through inlet channel

ACKNOWLEDGMENTS

This work was a product of research sponsored by the USACE-ERDC's Coastal and Hydraulics Laboratory (CHL) under contract No. W912HZ-06-C-0003. The authors would like to especially thank Dr. Nicholas C. Kraus, who is the manager of Coastal Inlets Research Program (CIRP) at CHL, ERDC, Vicksburg, MS, for his review of this paper. We thank CIRP team members Dr. Adele Militello Buttolph, Mitchell E. Brown, Kenneth J. Connell, Dr. Lihwa Lin, and Dr. Alan Zundel for collaboration on the CMS and SMS implementation during this 2-year development effort. We also

thank Dr. Xinya Ying in NCCHE for his help in producing numerical results of the long-term runs.

REFERENCES

Buttolph, A. M., Reed, C. W., Kraus, N. C., Ono, N., Larson, M., Camenen, B., Hanson, H., Wamsley, T., and Zundel, A. K. (2006). Two-dimensional depth-averaged circulation model CMS-M2D: Version 3.0, Report 2, sediment transport and morphology change. Technical Report ERDC/CHL-TR-06-7, US Army Engineer Research and Development Center, Vicksburg, MS.

Camenen, B., and Larson, M. (2005). A bedload sediment transport formula for the nearshore. *Estuarine, Coastal and Shelf Sci.*, 63, 249-260.

Camenen, B., and Larson, M. (2007). A unified sediment transport formulation for coastal inlet application. Contract Report ERDC/CHL CR-07-1, US Army Engineer Research and Development Center, Coastal and Hydraulics Laboratory, Vicksburg, MS.

De Vriend H.J., Zyserman J., Nicholson J., Roelvink J.A., Pechon P., and Southgate H.N., (1993). Medium-term 2DH Coastal Area Modeling. *Coastal Eng*., 21, 193-224.

Ding, Y., and Wang, S.S.Y. (2006a). Implementation of an efficient and accurate implicit solution scheme for the IMS-M2D hydrodynamic model. National Center for Computational Hydroscience and Engineering, University of Mississippi, Interim Contract Report for U.S. Army Engineer Research and Development Center, Coastal and Hydraulics Laboratory, February 2006.

Ding, Y., and Wang, S.S.Y. (2006b). Development of a numerical model for simulating tidal and wave-induced currents in coastal inlets. Proceedings of the Seventh International Conference on Hydroscience and Engineering, Philadelphia, PA, September 2006. <http://hdl.handle.net/1860/732>

Falconer, R. A. (1980). Modelling of planform influence on circulation in harbors. *Proc. 17th Coastal Eng. Conf.*, ASCE Press, NY, 2,726-2,744.

Kraus, N. C., and Larson, M. (1991). NMLONG: Numerical model for simulating the longshore current; Report 1: Model development and tests. Technical Report DRP-91-1, U.S. Army Engineer Waterways Experiment Station, Vicksburg, MS.

Lesser, G.R., Roelvink, J.A., van Kester, J.A.T.M., and Stelling, G.S. (2004). Development and validation of a three-dimensional morphological model. *Coastal Eng*. 51(8-9), 883-915.

Lin, L., Mase, H., Yamada, F., and Demirbilek, Z. (2006). Wave-action balance equation diffraction (WABED) model: Tests of wave diffraction and reflection at inlets. *Coastal and Hydraulics Engineering Technical Note, ERDC/CHL CHETN-III-73,* U.S. Army Engineer Research and Development Center, Vicksburg, MS.

Mellor, G.L. (1998). User guide for a three-dimensional, primitive equation, numerical ocean model, Princeton University, Princeton, NJ.

Militello, A., and Kraus, N.C. (2003). Numerical simulation of sediment pathways at an idealized inlet and ebb shoal. In: *Proc. Coastal Sediments* 03, CD-ROM publish by World Scientific Publishing (ISBN 981-238-422-7)

Militello, A., Reed, C.W., Zundel, A.K., Kraus, N.C. (2004). Two-dimensional depth-averaged circulation model M2D: Version 2.0, Report 1, Technical Documentation and User's Guide, ERDC/CHL TR-04-2, U.S. Army Engineer Research Development Center, Vicksburg, MS.

MIKE 21 (2006). MIKE 21 coastal hydraulics, hydrodynamic module – MIKE 21 HD – basic hydrodynamic module, Danish Hydraulic Institute, <http://www.dhisoftware.com/mike21/ Description/HD_module.htm>, (Jan 25, 2006).

Nishimura, H. (1988). Computation of nearshore current. In: *Nearshore Dynamics and Coastal Processes*, K. Horikawa, ed., University of Tokyo Press, Tokyo, Japan, 271-291.

Patankar, S.V. (1980). *Numerical heat transfer and fluid flow*. Hemisphere, NY, 1980.

Stone, H.L. (1968). Iterative solution of implicit approximations of multi-dimensional partial differential equations. *SIAM J. Num. Anal.*, 5(3), 530-558.

Zundel, A. K. (2006). Surface-water Modeling System reference manual. Brigham Young University – Environmental Modeling Research Laboratory, Provo, UT.

Zyserman, J.A., and Johnson, H.K. (2002). Modelling morphological processes in the vicinity of shore-parallel breakwaters. *Coastal Eng.* 45(3), 261–284.